5

Oxidation of graphitic surfaces

Reaction of oxygen with carbon surfaces is one of the simplest reactions involving elemental carbon. It is also the most important reaction which is the key to very diverse technological applications. The reaction of carbon with oxygen has been shown to play a decisive role in diverse fields such as the heterogeneous oxidation catalysis, the reentry shields in spacecraft research, and the solubility and functionalization of single-wall carbon nanotubes. In addition, the oxidation of carbon has been shown to drastically alter its physicochemical properties, such as the wettability, sticking and adsorption of the surface, and therefore, it serves as a powerful tool to tailor surface characteristics.

The carbon-oxidation reactions, when considered from the perspective of heterogeneous oxidation catalysis, have two functions. First, the reaction between carbon surfaces and oxygen is used to activate the carbon by increasing the surface area (hole-burning). Second, the reaction is used to introduce organic functional groups on to the carbon surfaces. These functional groups are those encountered in traditional organic chemistry reactions, for example carbonyl, carboxylic acid, etc. They are formed by the chemisorption of oxygen on carbon surfaces. It is their introduction on to the carbon surfaces which drastically alters the aforementioned physicochemical surface properties. Most importantly, these functional groups directly take part in surface reactions and therefore play a crucial role in heterogeneous oxidation catalysis. The stability and reactivity of the carbon-oxygen surface functional groups are important concerns for any catalytic oxidation reactions on carbon surfaces. Recently, porous carbon surfaces, especially carbon nanofibers, have shown to posses good catalytic properties [Geisler et al., 2003; Maximova, 2002]. However, the types of surface-oxygen functional groups and their stability still remain unknown.

Reaction of oxygen with carbon surfaces has been shown to have two main steps: The activation of molecular oxygen on the carbon surfaces, and the stabilization of the activated species by the formation of covalent bonds with the carbon atoms. However, in most of the collected data, the carbon surfaces are generally referred to as "coke" or "soot'. These terms were originally coined for any carbon residue obtained from the thermal cracking of hydrocarbons [Cornils et al., 2000; Schlögl, 1997]. This vague description does not consider the extreme structural diversity exhibited by carbon materials and, hence, causes a great deal of confusion. Also, a vast body of oxidation reactions has been carried out using liquid-phase oxidizing agents, such as permanganate ($KMnO_4$), nitric acid (HNO_3) etc. Oxidation by these reagents introduces foreign elements into the carbon matrix and, therefore, severely alters the intrinsic characteristics of the pristine carbon surfaces [Schlögl, 1997]. This is clearly demonstrated in the oxidation reaction involving permanganate which results in the intercalation of potassium within the graphitic layers of the sp^2 carbon structures [Chen et al., 1996]. Therefore, the data from such intercalated or doped carbon surfaces cannot directly be compared to the corresponding pristine carbon surfaces.

In this chapter, the oxidation of porous carbon surfaces, such as carbon nanofibers and colloidal graphite, by the oxidizing agent, hydrogen peroxide, will be examined. Two distinct advantages of hydrogen peroxide oxidation are: Oxidation can be achieved at ambient temperatures, and unlike other liquid-phase oxidizing agents, it does not incorporate foreign elements into the carbon surface. The thermal desorption of oxygen from the oxidized carbon surfaces is used to determine the oxygen binding energies. The desorption of carbon monoxide and carbon dioxide from the oxidized carbon surfaces are monitored to identify the surface functional groups. Chemisorption of oxygen on carbon surfaces depends on the surface structure, the availability of reactive sites, such as graphitic edge planes or defects, and also on the surface temperature. For example, graphite with nearly defect-free basal planes undergoes thermal oxidation only at extremely high temperatures. Low-temperature exposure to oxygen leads to only weakly physisorbed molecular oxygen, which has binding energies of around 0.12 eV. In the case of single-wall carbon nanotubes (SWNTs) also, the interaction with oxygen at ambient temperatures is of the van der Waals type, without any appreciable charge transfer. Oxidation studies of graphite and single-wall carbon nanotubes have indicated that exposure of oxygen to these surfaces initially leads to a physisorbed precursor state. Whether or not this proceeds to the formation of chemisorbed oxygen species largely depends on the presence of surface defects, temperature etc. Carbon nanofibers, on the other hand, have reactive edge planes and are therefore more susceptible to oxidation reaction. This chapter begins with an overview of physisorption and chemisorption of oxygen on carbon surfaces. The thermal desorption experiments involving oxygen, carbon monoxide and carbon dioxide from carbon nanofibers and colloidal graphite are

subsequently presented.

5.1. Physisorption of oxygen

Experimental studies on the exposure of graphite and SWNT to oxygen at ambient or low temperatures have proved that oxygen binds on these surfaces with a binding energy of 0.12 and 0.19 eV, respectively [Ulbricht et al., 2002b]. Also, in these experiments, the interaction of oxygen with graphite did not produce carbon monoxide or carbon dioxide as desorption products, as seen in the case of oxidative etching of graphite. Similarly, gradient-corrected and spin-polarized density functional calculations have shown the absence of any kind of charge transfer between O_2 and graphite [Giannozzi et al., 2003; Sorescu et al., 2001]. These studies suggested that that the dominant interaction of molecular oxygen with carbon is of van der Waals type. The reason for this non-reactivity is the energy mismatch of few tenths of an eV between the unoccupied states of O_2 and the valence band of graphite. Therefore, a transformation of the unoccupied oxygen state is required for any reaction between oxygen and the graphitic surface to occur. Lowering of the oxygen states is shown to be prevented by a kinetic barrier, which can be overcome, if the oxygen molecules are physisorbed on defect sites, such as vacancies, kinks or edge planes [Ulbricht et al., 2002b]. Therefore, materials, such as carbon nanofibers or colloidal graphite, are susceptible to chemisorption of oxygen due to the high density of defect sites (see section 3.2).

5.2. Chemisorption of oxygen

As mentioned in the previous section, the chemisorption of oxygen on graphitic surfaces requires the lowering of the unoccupied electron states in oxygen by binding to defect sites. This oxidation of graphitic surfaces below 600 °C is initiated by the adsorption on to defect sites. Above 700 °C, oxidation of graphite can happen by the etching of carbon atoms from the basal plane [Klusek et al., 2003]. Thermal oxidation, i.e., heating the graphite surface at temperatures typically between 600 and 1000 °C in an oxygen partial pressure between 10^{-4}–10^{2} mbar, is the most common technique for the oxidation of graphite [Bansal et al., 1971; Beck et al., 2002; Klusek et al., 2003; Loebenstein and Deitz, 1955].

However, this method has a serious setback as it generally leads to the uncontrolled depletion of surface carbon atoms in the form of carbon monoxide and carbon dioxide. The exposure of the carbon surfaces to oxygen at temperatures above 700 °C also results in the accumulation of undesired surface groups [Ehrburger and Vix-Guterl, 1998]. More controlled oxidation of the carbon surfaces can be carried out using low temperature liquid-phase oxidants, such as permanganate, perchlorate,

hydrogen peroxide, nitric acid etc. [Behrman and Gustafson, 1935; Chen et al., 1996]. However, the above oxidizing agents, excluding peroxide, introduce foreign elements into the graphite, and have been shown to alter the structural properties of the graphitic layers [Chen et al., 1996; Schlögl, 1997].

Two independent reaction mechanisms have been proposed for the oxidation of graphite surfaces: (1) reaction from the direct collisions of O_2 molecules with the reactive carbon sites [Eley-Rideal (ER) mechanism] and (2) the surface migration mechanism, i.e., the reaction with the migrating oxygen molecules that are first adsorbed on nonreactive sites (Langmuir-Hinshelwood [LH] mechanism) [Yang and Wong, 1981a,b]. The ER mechanism is initiated by the direct collision of the oxygen molecules with the graphitic defect sites. The reaction mechanism according to the LH formalism consists of two distinct steps: the physisorption of molecular oxygen on the graphitic basal surfaces, and the diffusion of these species to defect sites that subsequently results in the formation of carbon-oxygen surface functional groups [Schlögl, 1997]. These steps are presented in the following sections.

5.2.1. Mechanism of graphite oxidation

As pointed out above, the gas-solid reaction between molecular oxygen and a carbon surface can be modelled using either the Langmuir-Hinshelwood or the Eley-Rideal Mechanism. These mechanisms can be illustrated by considering the oxidation of a graphene sheet a the prototype for the carbon surface.

Implementing the LH mechanism, the oxidation of graphitic surfaces proceeds through two distinct steps: (1) adsorption of molecular oxygen onto the basal plane to form a physisorbed precursor state and (2) the surface diffusion of oxygen molecules to defect sites such as vacancies or edge planes [Schlögl et al., 1990]. The graphite surface sites involved in these two steps are illustrated in Fig. 5.1 as sites **A** and **C** respectively. The physisorption of an oxygen molecule, the first step, can be hypothetically represented as:

$$\mathbf{A} + O_2 \longrightarrow O_2(ads), \tag{5.1}$$

This interaction of molecular oxygen with a basal plane of graphite is physisorption in nature, without any charge-transfer [Ulbricht et al., 2002b]. On the basal plane, the charge transfer is prevented due to the kinetic barrier which is surpassed if the oxygen adsorbs on a defect site; the second step of the oxidation reaction [Dag et al., 2003]. This involves the surface diffusion of the physisorbed molecular oxygen to vacancies or edge sites **C**. Where it then undergoes a reduction to form species such as O_2^-, or O_2^{2-} and finally makes stable covalent bonds with the carbon atoms:

$$O_2(ads) + \mathbf{C} + 2e^- \longrightarrow O_2^{2-}(ads), \tag{5.2a}$$

$$O_2^{2-}(ads) + 2e^- \longrightarrow 2O^{2-}(ads), \tag{5.2b}$$

$$O^{2-}(ads) + \mathbf{C} \longrightarrow CO(ads) + 2e^-. \tag{5.2c}$$

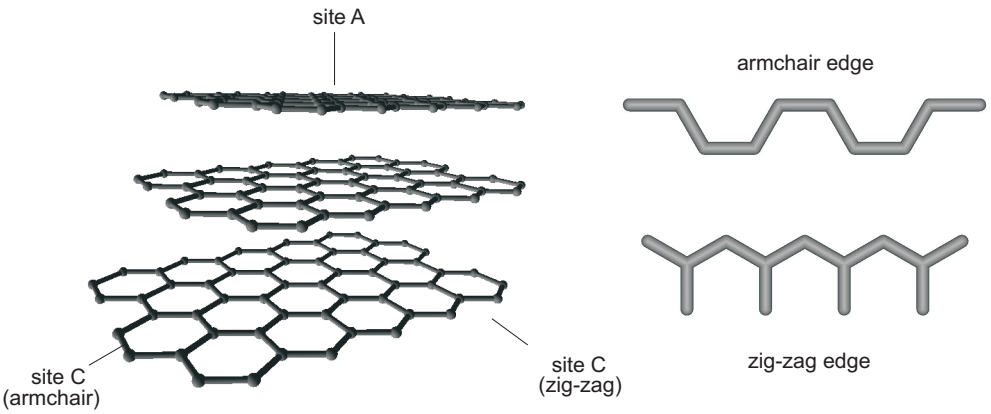

Figure 5.1.: Schematic illustration of the basal and edge planes in graphite: Site **A** is the part of an electron rich plane. Edge planes (site **C**) are highly reactive due to the partial saturation of valencies. Right panel: Two different types of sites can be identified on the edge plane: an arm-chair site and a zig-zag site. These two sites display different reactivity with activated oxygen species, and results in different polyfunctional organic surface groups.

The site **C**, as indicated in Fig. 5.1 (right panel), presents two alternatives in a the reactive edge plane : a "zig-zag" or an "arm-chair" site [Blyholder and Eyring, 1959]. The reduction of an oxygen molecule to an oxide (O^{2-}) ion, as depicted in Eqs. (5.2a) and (5.2b), is not the only possibility. In electron paramagnetic experiments it has often been found that other ionic species, such as peroxide (O_2^{2-}) or superoxide (O_2^{-}) ions, co-exist on the surface [Atamny et al., 1992; Bielański and Haber, 1991; Schlögl and Boehm, 1983]. The complete reduction of oxygen to oxide ion is based on the argument about the relative surface stability of the oxide ion. The relative stability of various oxygen species in the gas phase, on a solid surface, and in a lattice is shown schematically in Fig. 5.2.

This two-stepped reaction mechanism (LH) is used to explain the oxidation of graphitic basal planes, and therefore it can also be used to explain the oxidation of a colloidal graphite surface. However, for materials such as carbon nanofibers whose exterior surfaces are characterized by highly reactive edge planes (see Fig. 3.5 in chapter 3), oxidation does not necessarily require physisorption. Thus, the oxidation mechanism of carbon nanofibers, involves only a single step, which is the Eley-Rideal mechanism. In this mechanism, the oxidation of a carbon surface happens by the direct collision of an oxygen molecule with the reactive edges (armchair or zig-zag) of graphene sheet [Yang and Wong, 1981a]. Oxygen molecules approaching these planes are reduced by charge transfer from the carbon atoms in these planes. The resulting intramolecular Coulomb repulsion breaks the O—O bond exothermically without an activation barrier, and results in the formation of carbon-oxygen functional groups

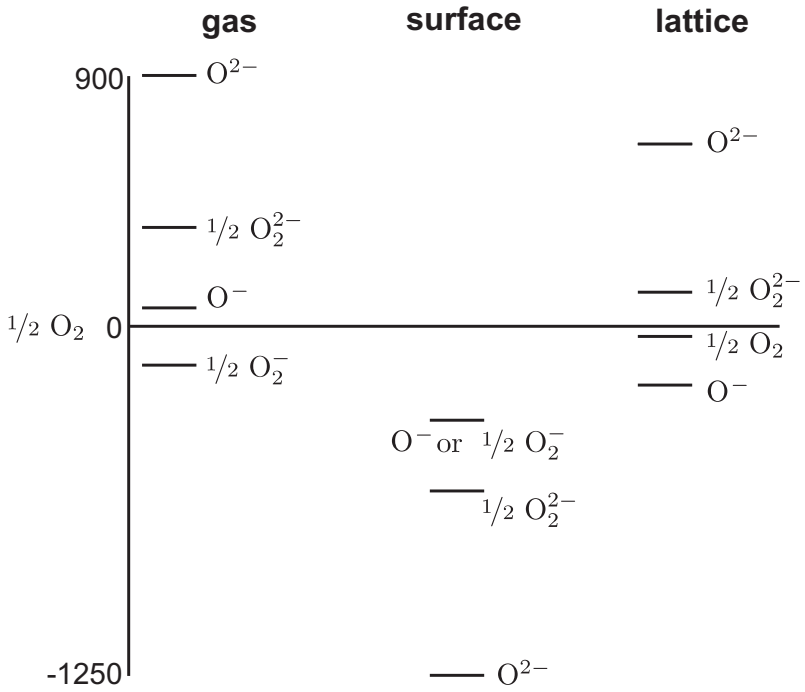

Figure 5.2.: The relative stability of various activated oxygen species in gas phase, on a surface, and within a lattice, with respect to $\frac{1}{2}O_2$ in the gas phase [Gellings and Bouwmeester, 2000]. Due to the extreme stability of O^{2-} on the surface, this species is formed preferentially and combines with reactive sites to form surface-functional groups. The plot is not to the scale.

[Hahn et al., 1999].

5.2.2. Carbon-oxygen surface functional groups

The reaction of activated oxygen species with carbon at site **C** results in the formation of carbon-oxygen surface functional groups, which can be represented as:

$$O^{2-}(ads) + \mathbf{C} \longrightarrow CO(ads) + 2e^-. \tag{5.3}$$

The adsorbate $CO(ads)$ in the above reaction is a carbon-oxygen surface group. Typical groups observed on oxidized carbon surfaces are carboxylic acid, acid anhydride, quinone etc., and are shown in Fig. 5.3. The multitude of functional groups formed on carbon surfaces is due to different reactivity of the two different types of edge sites (Fig. 5.1). Carbon-oxygen surface functional groups determine the many physicochemical properties of the carbon surfaces, such as surface acidity, sticking, wetting etc. These functional groups play a crucial role in the field of heterogeneous catalysis. One example is the partial oxidation of ethylbenzene on carbon surfaces [Ehrburger and Vix-Guterl, 1998]. The surface concentrations of the carbon-oxygen

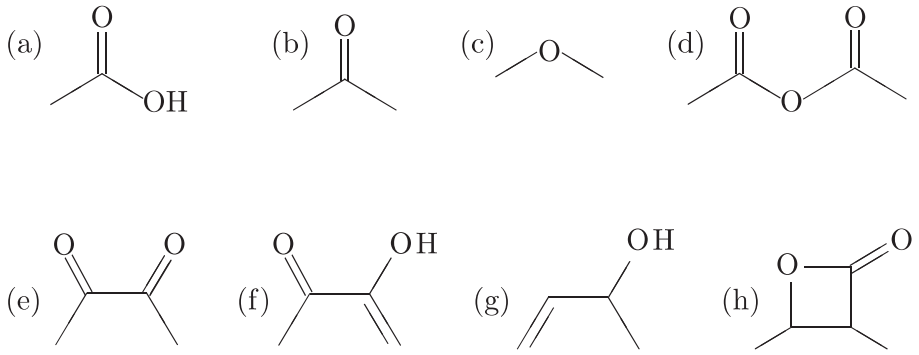

Figure 5.3.: Typical surface functional groups observed after oxidation of carbon surface: (a) carboxylic acid, (b) keto, (c) ether, (d) anhydride, (e) quinone, (f) phenolic, (g) hydroquinone or (h) lactone.

surface groups are temperature dependent. Their ease of formation and stability are of paramount importance in the field of heterogeneous catalytic regeneration [Schlögl, 1997; Szymański et al., 2002; Toebes et al., 2004; Zielke et al., 1996a,b]. Consequently, their detection and population have been studied classical chemical detection methods, vibrational spectroscopy, thermal desorption spectroscopy and photoelectron spectroscopy. All the above techniques have limitations in assessing the identity of surface functionalities, and they are generally used in combinations with each other. The use of chemical detection methods, such as neutralization and esterfication reactions of acidic and anhydride groups are based on the identification

Table 5.1.: Decarbonylation and decarboxylation reactions from the classical organic chemistry point of view along with the corresponding pyrolytic elimination temperatures.

Surface group	Product	Temperature	References
Carboxylic acids	CO_2	453–573 K	[Pun, 1987]
Acid anhydrides	CO, CO_2	673–720 K	[Moreno-Castilla et al., 1998]
		710–930 K	[Nevskaia et al., 1999]
Lactones	CO_2	410–430 K	[Adam et al., 1972]
		463–923 K	[Marchon et al., 1988]
Peroxides	CO_2	823–873 K	[Marchon et al., 1988]
Phenol	CO	873–973 K	[Figueiredo et al., 1999]
Quinones	CO	1073–1173 K	[Marchon et al., 1988]

of corresponding dissociation constants. Therefore, they can be used only in situations where these constants are centered around discreet values. The complexity of these chemical techniques increases when the surface functional groups start to react with each other. Photoelectron spectroscopy uses the O1*s* signal to identify the functional groups. However this method is insensitive to small variations in the chemical environment, and therefore is not frequently employed. Thermal desorption spectroscopy (TDS) and vibrational spectroscopy are more often used techniques, and the use of TDS also helps to measure the thermal stability of these surface functional groups. In thermal desorption spectroscopy the temperatures at which carbon dioxide and carbon monoxide desorbed from the surface are compared with decarbonylation and decarboxylation reactions (i.e., the elimination of CO and CO_2) in classical pyrolytic elimination reactions. A compilation of desorption temperatures of carbon monoxide and carbon dioxide that have been obtained using thermal desorption studies from carbon surfaces are presented in Table 5.1. It is important to note that often this data is obtained from different types of carbon materials. In addition, they decomposition temperatures strongly depend on the chemical treatment of the carbon surfaces. One functionality of particular interest is the quinone functional group (Fig. 5.3). This is because the oxidation of polyaromatic hydrocarbons (PAHs) with hydrogen peroxide is shown to yield quinones [Schumb et al., 1955]. Due to similarities between the PAH and graphitic basal planes, a similar reaction should result in the formation of quinone surface functional groups.

5.3. Temperature programmed oxidation of carbon surfaces

In this section, the oxidation of colloidal graphite and carbon nanofibers using hydrogen peroxide (H_2O_2) is presented. The first part deals with the desorption of oxygen from carbon surfaces. The binding energy of oxygen on the carbon surface is determined from desorption spectra. In the second part, the thermal desorption of carbon monoxide and carbon dioxide from the oxidized carbon surfaces are monitored. The identity of the functional groups are then determined by comparing the desorption temperature with the temperature corresponding to the pyrolytic elimination reaction given in the Table 5.1.

5.3.1. Thermal desorption of hydrogen peroxide

As pointed out earlier, the oxidation of the carbon surfaces at low temperatures can be achieved using hydrogen peroxide. It does not introduce any foreign elements into the carbon sample (the introduction of hydrogen into the carbon samples generally is observed to saturate the dangling bonds) [Behrman and Gustafson, 1935; Puri and Kalra, 1971]. In aqueous solutions, hydrogen peroxide decomposes slowly into

water and oxygen, according to the following equilibrium:

$$2H_2O_2 \rightleftharpoons 2H_2O + O_2.$$

The disproportionation of the hydrogen peroxide is believed to involve chain reactions, and the equilibrium shifts to right in the presence of catalytic metal surfaces. However, it is understood that except at high temperatures in vapor phase, the above conversion does not usually occur without the presence of a catalytic surface. To further slowdown the conversion, peroxide is stored below room temperature.

Carbon nanofibers (Applied Science Inc. Cedarville, USA) and colloidal graphite (Agar Scientific, Essex) are made into an aqueous dispersion, and films of these materials are made by spray-coating them on to a tantalum disc of the sample holder (see chapter 3 for further experimental details of sample preparation). After removing excess solvent (water) by resistive heating to 100 ℃, the tantalum disk is mounted inside a ultrahigh vacuum (UHV) chamber. Before thermal desorption experiments, the sample surfaces are outgassed by repeated heating to 1100 K, so that desorption due to chemisorbed impurities, such as oxygen, carbon dioxide, carbon monoxide and water, is diminished. The sample surface is cooled down to 77 K by a connection to a liquid nitrogen cryostat. Hydrogen peroxide used for the desorption experiments is obtained from Solvay Interox GmbH (60 % aqueous solution). Any dissolved gas-phase impurities are removed from the hydrogen peroxide by a series of freeze-pump cycles. Residual gas analysis of hydrogen peroxide indicates a prominent peak at m/e = 32 a.m.u/e which corresponds to the oxygen and another peak of water (m/e = 18 a.m.u/e). However, this residual gas analysis showed no contributions from carbon monoxide or dioxide, indicating that peroxide undergoes cracking at the QMS ion source. On the other hand, when the carbon surface is dosed with peroxide, as in the thermal desorption experiments, the desorption peaks corresponding to the evolution of carbon monoxide and dioxide are obtained. Therefore, it is concluded that when peroxide is dosed on to the carbon surface, it undergoes decomposition to oxygen and water. A typical exposure series of hydrogen peroxide is obtained by dosing the sample surface with an initial coverage of hydrogen peroxide of up to 3 L. After each exposure, the thermal desorption spectra of oxygen (m/e = 32 a.m.u/e), water (m/e = 18 a.m.u/e), carbon monoxide (m/e = 28 a.m.u/e) and carbon dioxide (m/e= 44 a.m.u/e) are recorded using a constant heating rate of 1 K s^{-1}.

The thermal desorption (TD) spectra of oxygen desorption from carbon nanofibers for three different exposures of hydrogen peroxide are displayed in Fig. 5.4. The temperature of the spectra is calibrated using the thermal desorption spectra of xenon multilayers from the surface of a single graphite crystal [Ulbricht et al., 2002a]. Oxygen desorption from carbon nanofibers is characterized by very broad desorption traces with a peak maximum appearing in the range of 550 and 650 K (for the exposure 0.4 L). This broadening is also seen to increase with

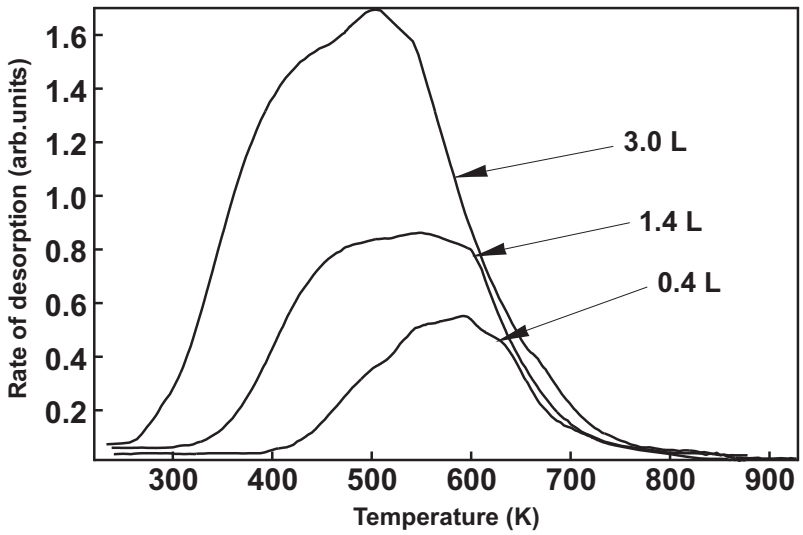

Figure 5.4.: Series of thermal desorption spectra of molecular oxygen (m/e= 32 a.m.u./e) obtained after exposing a thin film of carbon nanofibers to three different exposures of hydrogen peroxide (0.4, 1.4 and 3.0 L). The exposure is made at 77 K, and the spectra are recoded with a heating rate of $1\,\mathrm{K\,s^{-1}}$.

the exposure. The broadening of the thermal desorption spectra, from surfaces of porous materials, is in general explained by the dominant diffusion processes of gas molecules within the inner void spaces of the porous substrates [Ulbricht, 2003]. In porous carbon materials, it has been shown that the desorption profile has a mass transport contribution from the internal void regions (see chapter 2 for more details). Also, inhomogeneity of the sample surface can slow down the desorption process which further contributes to desorption peak broadening. This is especially likely, as we observe a progressive broadening of the peaks with increasing exposure to peroxide. When compared to oxygen desorption temperatures from single-wall carbon nanotube bundles, the desorption from carbon nanofibers occurs at a remarkably higher temperature [Ulbricht, 2003; Ulbricht et al., 2003]. The desorption temperature of oxygen maximum at 600 K, here, is more likely due to the chemisorption of oxygen [Schlögl, 1997]. This high temperature desorption feature is totally absent in the case of carbon nanotube bundles, where the interaction between molecular oxygen and the carbon surface is predominantly a weak van der Waals type. The susceptibility of carbon nanofibers to oxidation can be ascribed to the reactive edge planes as well as greater defect densities that are present. The strong chemisorptive interaction of oxygen on carbon nanofibers is further evident by the desorption of carbon monoxide and carbon dioxide (see 5.3.2). In addition, the thermal desorption spectra are found to be not reproducible unless a new sample surface is used, which indicates an irreversible surface oxidation upon exposure to peroxide. However, similar peak broadening is absent for the thermal

desorption of non-reactive gases. For example, the TD spectra of SF_6 before and after surface oxidation is shown in Fig. 5.5, where no visible differences between the TD spectra before and after oxidation can be seen. The TD spectra of oxygen

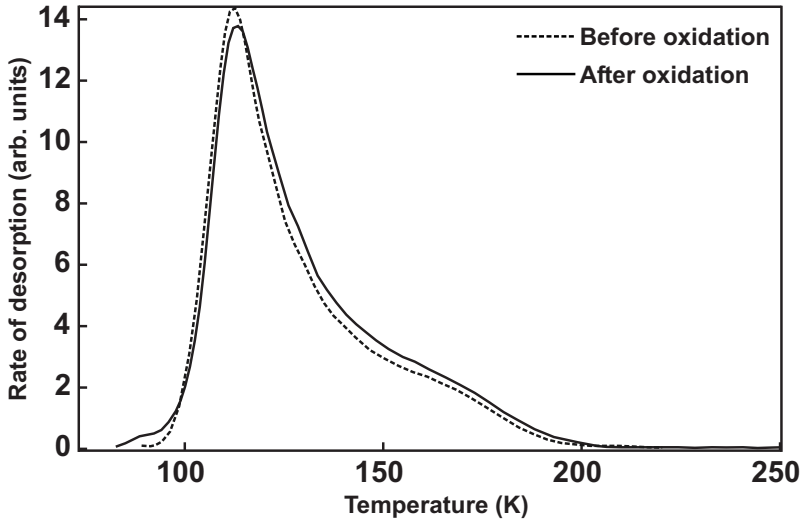

Figure 5.5.: Thermal desorption spectra of SF_6 (m/e = 127 a.m.u./e) from carbon nanofibers before (broken lines) and after (solid line) oxidation experiments, for an exposure of 0.5 L. The spectra are recorded with a heating rate of $1\,\mathrm{K\,s^{-1}}$.

desorption from colloidal graphite surface after an of exposure of up to 12.7 L is displayed in Fig. 5.6. They show two distinct features: a low temperature desorption peak, which appears at 110 K, and a high temperature feature with peak maximum appearing between 400 and 800 K. The temperature for the maximum desorption rate, T_{max}, in the low temperature desorption feature shifts to lower temperatures with increasing coverage. The activation energy corresponding to this desorption feature is calculated using the Falconer-Madix analysis [Falconer and Madix, 1977]. In this method, the activation energy of desorption is derived from the logarithmic form of Arrhenius rate equation (for details of this method, see chapter 3):

$$\ln\left(-\frac{d\theta}{dt}\right) = \ln(\nu) + n\ln(\theta) - \frac{E_d^{\ddagger}}{k_B T}, \tag{5.4}$$

where ν is the pre-exponential frequency factor, n is the order of desorption and $E_d^{\ddagger}$ is the activation energy of desorption. Using the above equation, the isotherms (*logarithm of rate* versus *logarithm of surface coverage*) are constructed at a series of constant temperatures. These plots are have the intercept, I, given by:

$$I = \ln(\nu) - \frac{E_d^{\ddagger}}{k_B T} \tag{5.5}$$

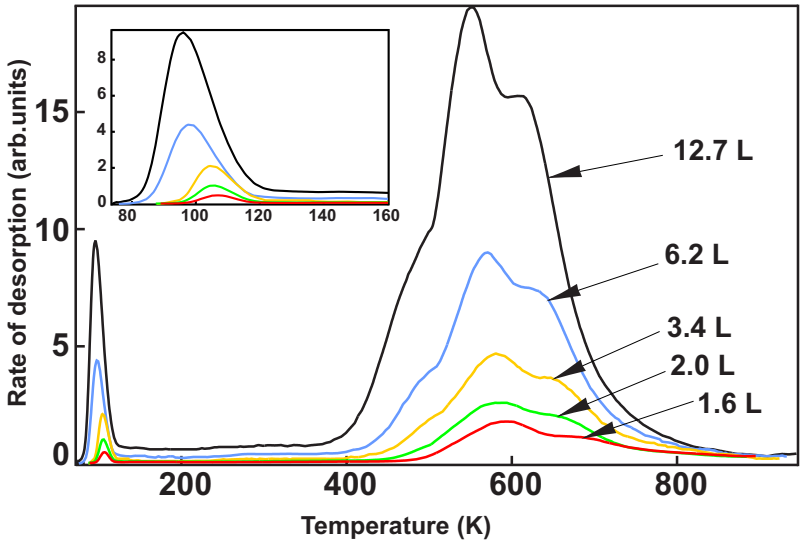

Figure 5.6.: Series of thermal desorption spectra of molecular oxygen (m/e = 32 a.m.u./e) obtained after exposing colloidal graphite surface with hydrogen peroxide for a coverage of up to 12.7 L. The inset shows an expanded view of the low temperature desorption feature.

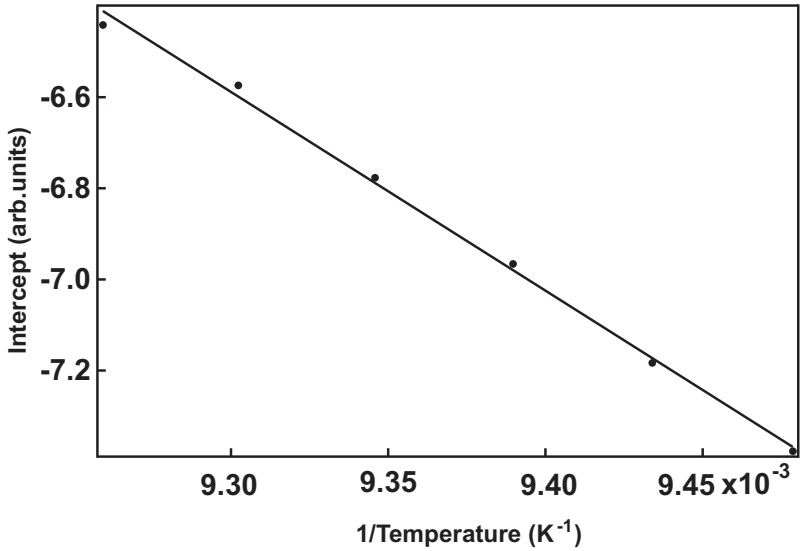

Figure 5.7.: Intercept plot for thermal desorption of oxygen from colloidal graphite constructed from the isotherms between 95 and 105 K.

Using the intercepts and corresponding temperature of isotherms, a plot of I versus $1/T$ is made (Fig. 5.7). From Eq. (5.5), the pre-exponential frequency factor and activation energy for oxygen desorption are obtained from the slope and the intercept of the linear fit in the intercept plot. The activation energy for desorption has a

value of 0.35 ± 0.02 eV. A similar desorption feature has been observed when oxygen was exposed to graphite powder at 78 K, and it has been shown that this peak arises from weakly chemisorbed peroxo- ligand (O_2^{2-}) [Atamny et al., 1992; Schlögl et al., 1990]. The pre-exponential frequency factor for the desorption of this moiety is found to be $2.8 \times 10^{14\pm1}\,s^{-1}$. The desorption feature corresponding to the peak maxima at 600 K shows a shoulder feature which becomes increasingly prominent with coverage. Since T_{max} of this peak is observed to be a constant over coverage of up to 15 L or more, the corresponding binding energy is derived using Redhead's peak maximum method [Redhead, 1962]. This is done according to the the following equation:

$$E_d^{\ddagger} = k_B T_{max}[\ln(\nu T_{max}/\beta) - 3.64]. \tag{5.6}$$

Here, β is the heating rate. Use of this equation is generally valid for the first-order desorption. However, it can be extended to the evaluation of thermal desorption spectra corresponding to a different order, if the T_{max} used in the analysis is obtained from a completely saturated monolayer. Due to only a very weak coverage dependence of T_{max}, the Redhead equation can be used to derive the activation energy: 1.81 ± 0.11 eV.

A comparison between the desorption features of oxygen from carbon nanofibers and those from colloidal graphite reveals that in colloidal graphite oxygen also binds to a low binding energy basal plane. The reaction, therefore seems to proceed via a two-step reaction mechanism (Langmuir-Hinshelwood mechanism). On the other hand, the single broad desorption feature from carbon nanofibers indicates that the reaction proceeds through a single-stepped mechanism (Eley-Rideal). The charge transfer and the formation of carbon-oxygen functional groups by the single-step mechanism (ER) can be envisioned similar to reactions of polyaromatic hydrocarbons (PAH). The justification for this comparison is the structural and electronic similarity between PAHs and graphene sheets. The oxidation of polyaromatic hydrocarbons with hydrogen peroxide is shown to produce quinones [Fig. 5.3(e)] [Schumb et al., 1955]. The single step reaction between oxygen molecule and carbon atoms

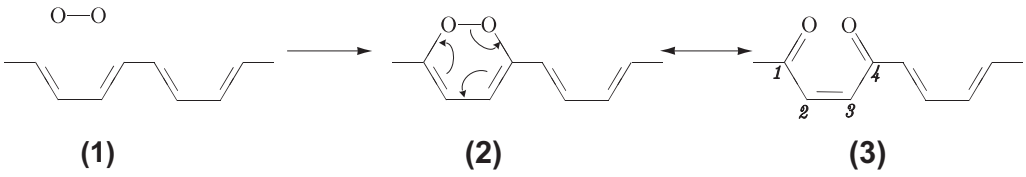

Figure 5.8.: Illustration of the ER mechanism between molecular oxygen and an armchair edge of a graphene sheet. The chemisorption of molecular oxygen on the armchair edge leads to the formation of aromatic peroxide (2) which rearranges to form a *1,4*-quinoid functional group (3). Curved arrows in step 2 indicate the direction of electron transfer [Gleicher, 1974; Zhu et al., 2000]

of the reactive edge is illustrated in here by considering an arm-chair edge as an

example [Fig. 5.8)]. The reaction is assumed to proceed through two elementary steps as shown in the figure. The first step (1) involves the chemisorption of oxygen molecule on the arm-chair, which results in the formation of an aromatic peroxide surface functional group (2). This surface group undergoes a rearrangement and lead to the formation of a *1,4*-quinoid surface functional group (3).

5.3.2. Decarbonylation and decarboxylation of carbon surfaces

During the thermal desorption of oxygen, the carbon-oxygen surface functional groups formed by the oxidation of the carbon surfaces also undergo the elimination of carbon monoxide and carbon dioxide. The temperature dependence of these elimination reactions can be compared to decarbonylation (i.e., the elimination of carbon monoxide) and decarboxylation (i.e., the elimination of carbon dioxide) in traditional organic chemistry [Lizzio et al., 1990; Radovic et al., 1991]. Therefore, it is possible to establish the identity of the surface-functional groups by comparing the desorption temperatures of carbon monoxide and dioxide with the decarbonylation and decarboxylation reactions in organic chemistry. The depletion of surface carbon in the form of carbon monoxide and dioxide can be hypothetically represented in the following set of equations [Schlögl, 1997]:

$$\mathrm{CO}(ads) \longrightarrow \mathrm{CO}(gas) + \mathbf{C}, \tag{5.7a}$$

$$\mathrm{O}^{2-}(ads) + \mathrm{CO}(ads) \longrightarrow \mathrm{CO_2}(ads) + 2\mathrm{e}^{-}, \tag{5.7b}$$

$$\mathrm{CO_2}(ads) \longrightarrow \mathrm{CO_2}(gas) + \mathbf{C}, \tag{5.7c}$$

where **C** is the site corresponding to the edge plane of the graphene sheet. The complete oxidation of a primary CO complex to carbon dioxide, as shown in Eq. (5.7b), is possible when the complex is thermally stable. The thermal desorption spectra of carbon monoxide and carbon dioxide desorption from oxidized carbon nanofibers and colloidal graphite are displayed in Figs. 5.9 and 5.10, respectively. They are recorded after exposing the carbon samples to a peroxide coverage equivalent to 0.5 and 12.7 L respectively, and using heating rate of $1\,\mathrm{K\,s^{-1}}$. CO desorption from oxidized carbon nanofibers [Fig. 5.9(a)] exhibits complex thermal desorption peaks which have an onset at 420 K. Two peaks with their maxima at 500, and 540 K are seen to merge with another peak that is centered at 620 K. The high temperature peak is seen to extend up to 700 K where it joins with desorption contributions from the background. By comparing the desorption temperatures of these peaks with the temperatures given in Table 5.1, it can be concluded that the carbon monoxide desorption is due to the presence of carboxylic anhydride surface group [Fig. 5.3(d)]. The desorption spectra of carbon dioxide [Fig. 5.9(b)] from the oxidized carbon nanofibers indicate a feature that starts at 344 K has a peak maximum at 430 K. Two additional peaks are seen at 495 and 540 K. The temperatures of these desorption peaks are in the range of thermal decomposition of carboxylic acid and lactone functional groups [Fig. 5.3(a)

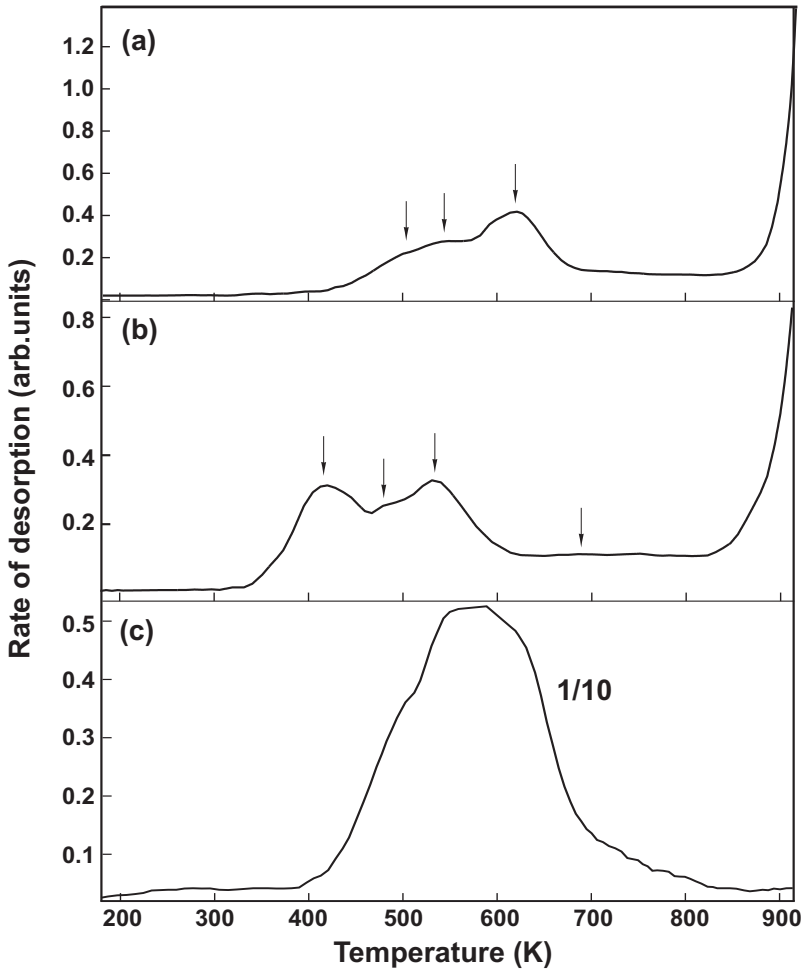

Figure 5.9.: Thermal desorption spectra of (a) CO and (b) CO_2 after exposing carbon nanofibers with 0.5 L of hydrogen peroxide. The oxygen trace (c) is scaled down by a factor of 10 for comparison. For the temperatures above 800 K, the spectra are characterized by the desorption of carbon monoxide and dioxide from the background. The heating rate for all the three spectra is $1\,K\,s^{-1}$.

and (h), respectively]. The evolution of carbon dioxide and carbon monoxide at temperatures which are close to each other is generally due to the presence of acid anhydrides. This is because anhydrides undergo successive elimination reactions producing carbon dioxide and carbon monoxide. The contribution that arises from the decomposition of surface functional groups (quinones and phenols) at temperature above 900 K is not analyzed due to the rising background.

The carbon monoxide desorption spectra from oxidized colloidal graphite are displayed in Fig. 5.10(a). The two peaks having a maximum at 570 and 600 K are assigned to the decomposition of this acidic functional group. The carbon dioxide desorption spectrum [Fig. 5.10(b)] also indicates two closely spaced peaks at 610 and

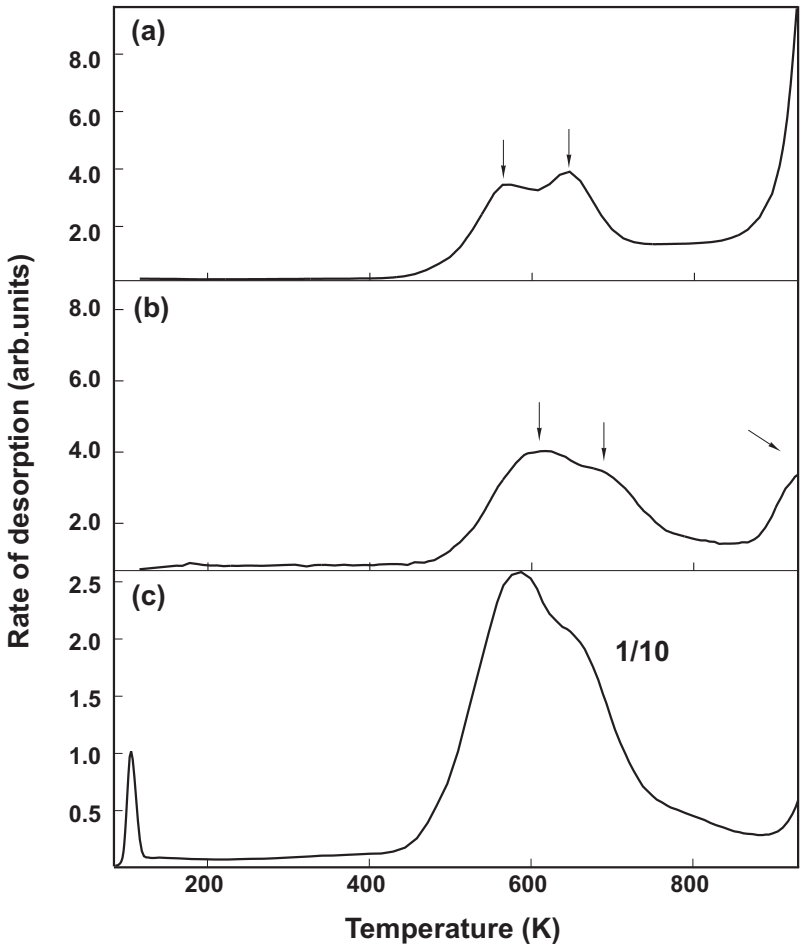

Figure 5.10.: Thermal desorption spectra of (a) CO and (c) CO_2 after exposing colloidal graphite with 12.7 L of hydrogen peroxide. The oxygen trace (c) is scaled down by a factor of 10 for comparison. For the temperatures above 800 K, the spectra are characterized by the desorption of carbon monoxide and dioxide from the background. The heating rate for all the three spectra is $1\,K\,s^{-1}$.

690 K. These fall in the same temperature range as those of the carbon dioxide desorbing from carbon nanofibers. Additionally, a peak is observed near 900 K whose origin is attributed to either lactone (463–923 K) or phenol (873–973 K) or both.

5.4. Summary and outlook

The oxidation of carbon nanofibers and colloidal graphite was carried out using hydrogen peroxide. Thermal desorption spectra of oxygen from the oxidized carbon nanofibers exhibits a broad peak, having a peak maximum at 600 K. The peak broadening observed in the desorption spectra increases with higher exposure to per-

oxide. This suggests that the broadening is a result of inhomogeneities that develop during the irreversible oxidation process. No attempt was made to calculate the corresponding binding energy due to the extremely broad desorption feature. The TD spectra of oxygen from colloidal graphite shows two distinct desorption features: a low temperature desorption peak at 110 K, and a high temperature desorption peak which has a complex doublet structure. The activation energy of desorption and the pre-exponential frequency factor corresponding to the desorption peak at 110 K are calculated to be 0.35 ± 0.02 eV and $2.8 \times 10^{14\pm1}\,s^{-1}$, respectively. The activation energy of desorption for the 600 K peak is 1.81 ± 0.11 eV. A comparison of the features in the oxygen desorption spectra from the surfaces of colloidal graphite and those from carbon nanofibers suggests that, in colloidal graphite, the oxidation proceeds via the physisorption of oxygen on the basal plane, which then migrates to reactive edge planes (Langmuir-Hinshelwood mechanism). While, the features of oxygen desorption from carbon nanofibers indicates that chemisorption occurs with a direct collision on exposed reactive edge planes (Eley-Rideal Mechanism).

Thermal desorption spectra of carbon monoxide and carbon dioxide from oxidized carbon nanofibers and colloidal graphite show complex desorption features, all of which are below 700 K. From the desorption spectra of carbon monoxide and carbon dioxide, I have identified that most of the surface groups are acidic functionalities, such as carboxylic acid, acid anhydrides and lactones. However, a more detailed study is required in order understand the high temperature desorption features. In particular, the desorption temperatures above 1000 K where the carbon monoxide desorption from quinone functionalities is expected.